

# Characterization of epitaxial Cr thin films

CJ Sheppard<sup>1</sup>, ARE Prinsloo<sup>1</sup>, PR Fernando<sup>1</sup>, ZP Mudau<sup>1</sup>, AM Venter<sup>2</sup> and EE Fullerton<sup>3</sup>

<sup>1</sup>Department of Physics, University of Johannesburg, PO Box 524, Auckland Park, 2006

<sup>2</sup>Research and Development Division, Neca Limited, P.O. Box 582, Pretoria 0001, South Africa

<sup>3</sup>Center for Magnetic Recording Research, University of California, San Diego, 9500 Gilman Dr., La Jolla, CA 92093-0401, USA

Author e-mail address: [alettap@uj.ac.za](mailto:alettap@uj.ac.za)

**Abstract.** Thin films and heterostructures of Cr and Cr alloys show fascinating properties that is not observed in the bulk material and research into their magnetic properties gives insight into dimensionality effects in these materials. This paper reports on the characterization of Cr thin films on MgO(100), MgO(110) and fused silica substrates, of thicknesses 20nm to 320nm. X-ray diffraction (XRD) results showed good epitaxial growth for films prepared on the single-crystalline MgO substrates, with Cr(002) and Cr(211), whilst those prepared on the polycrystalline fused silica were polycrystalline. The mosaicity and coherence length were determined from the XRD results. Standard four-point probe measurements were performed to obtain the resistance ( $R$ ) of the films as function of temperature ( $T$ ) the anomaly in the  $\rho(T)$  curves was used to determine the Néel temperature ( $T_N$ ).  $T_N$  versus  $t$  graphs for the various substrates show the behaviour expected for the samples prepared on MgO(110) and fused silica substrates, but rather unique behaviour is seen in this curve for samples prepared on MgO(100). This might be attributed to internal strain effects in these thin films.

## 1. Introduction

Cr and Cr alloy systems exhibit a large variety of antiferromagnetic properties and constitute a class of systems that undergoes magnetic phase transitions associated with the extent of nesting between the hole and conduction bands of the Fermi surface [1, 2]. The interest into the properties of these materials originates from their spin-density-wave (SDW) state which is directly linked to the nested Fermi surface and which contributes to nearly all the magnetic properties of Cr [1, 2].

Bulk Cr is an itinerant antiferromagnet that forms an incommensurate (I) SDW below its Néel temperature ( $T_N$ ) of 311 K. The ISDW is characterized by a temperature dependent wave-vector  $\mathbf{Q}$  determined by the nesting of the Fermi surface along the  $\langle 001 \rangle$ -directions [2]. The ISDW period varies from 78 Å at  $T_N$  to 60 Å at 10 K. This bulk behaviour is easily perturbed by strain or impurities that can alter  $T_N$ , the spin directions, the ISDW period, or drive the magnetic order to be commensurate with the lattice, resulting in a CSDW phase [1, 2]. In view of this, previous research in this field therefore suggests that once the fundamental role of the SDW in the properties in these materials is understood, the alloy can be tailored to give physical properties that can be useful in practical applications [1, 3].

Taking this into consideration, significant research interest exists into the physical properties of dilute Cr alloys, specifically in their role as spacer layers in magnetic multilayer thin film structures [3-7]. Results obtained have revealed fascinating properties not previously observed in bulk materials, including giant magnetoresistance [3-8]. Since specific magnetic properties can be tailored and designed in artificially structured materials this makes them useful for practical applications. The magnetic ordering of Cr near surfaces, or in thin layers have also rendered interesting fundamental problems [3-7]. Thus the study of SDW effects of Cr and its alloys when confined in thin films and multilayer structures provides a fascinating experimental test bed and such studies will contribute valuable information on dimensionality effects on the behaviour of Cr and Cr alloys.

This project is aiming to link the magnetic properties of Cr and Cr alloy thin films with stress and strain in these films, this paper reports on the magnetic properties of epitaxial and polycrystalline Cr thin films.

## 2. Experimental

The Cr films were prepared using DC magnetron sputtering at 800°C from an elemental source onto single-crystal MgO(100), MgO(110) and polycrystalline fused silica substrates. This respectively renders epitaxial and polycrystalline Cr thin films, respectively. Films were prepared in a thickness series with thickness ( $t$ ) varying between 20 and 320 nm. Each film structure was characterized using X-ray diffraction (XRD) techniques. Electrical resistance measurements, using standard DC four-probe methods, were employed to determine the Néel transition temperatures ( $T_N$ ) for these films.

## 3. Results

Figures 1(a), (b) and (c) show representative XRD results for the Cr thin films prepared on MgO(100) with  $t = 40$  nm, MgO(110) with  $t = 40$  nm and polycrystalline fused silica substrates with  $t = 320$  nm, respectively. The results indicate that the samples prepared on the MgO(100) and MgO(110) are indeed epitaxial exhibiting a single crystallographic orientation, with the Cr layers showing preferred growth directions of (100) and (211), as is indicated in figure 1(a) and (b). Samples prepared on polycrystalline fused silica substrates did not deposit with preferred growth orientation, but show a polycrystalline crystalline structure, as is seen in figure 1(c).

XRD results from the thin films prepared on MgO(100) and MgO(110) substrates enabled determination of the lattice parameters, the coherence length (length scales over which the films are structurally coherent [9] along the growth direction, analyzed from the full-width at half-maximum (FWHM) of the Bragg peaks in conjunction with the Debye-Scherrer formula after removing the instrumental resolution) and the mosaic spread obtained from the FWHM of the rocking curves [9]. Assessment of the results summarized in Table 1 reveals that for the films on the MgO(100) the mosaicity decreases and the coherence length increases slightly with thickness. Samples prepared on the MgO(110) show no clear general trend in the mosaicity though the coherence length increase slightly as function of Cr thickness. This indicates a general trend of improved crystallite alignment with film thickness [7, 9]. It is also noted that for the 320 nm Cr samples on both the MgO(100) and MgO(110) substrates, the mosaicity and coherence length have weaker correlation compared to the 160 nm thick film.

The Néel temperatures ( $T_N$ ) of the films were determined from anomalies observed in electrical resistance ( $R$ ) measurements as a function of temperature ( $T$ ). Representative examples of measured  $R - T$  curves are shown in figures 2(a), (c) and (d) for films with  $t = 160$  nm on the MgO(100) substrate,  $t = 40$  nm on MgO(110) and  $t = 80$  nm on polycrystalline fused silica, respectively. Anomalies in the form of humps are observed in the  $R - T$  curves of the samples prepared on the MgO(100) and MgO(110) substrates. This behaviour is associated with the formation of the SDW on entering the antiferromagnetic phase on cooling through the Néel temperature ( $T_N$ ) [1]. The sudden increase in resistivity on cooling through  $T_N$  finds its origin in the nesting of electron and hole Fermi surfaces [1].

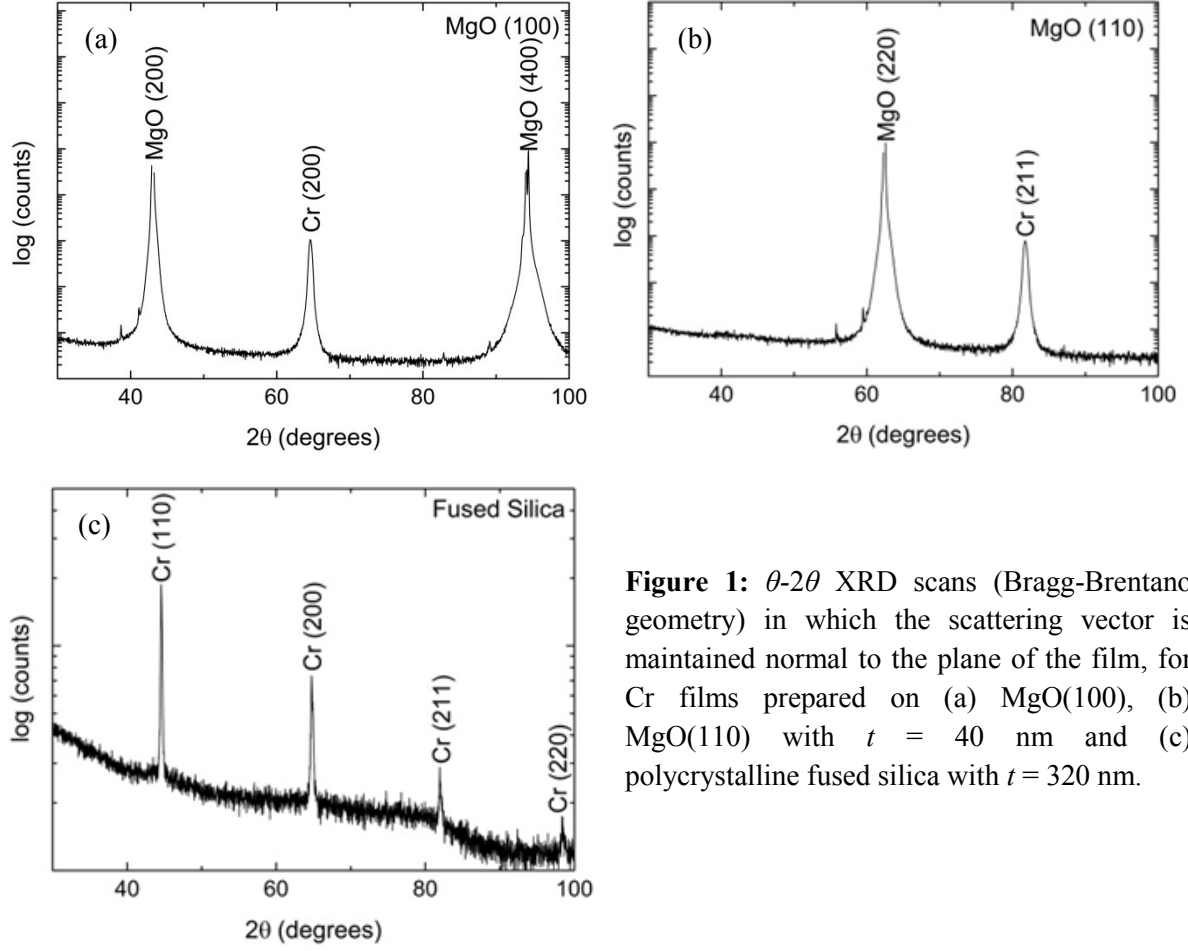


**Figure 1:**  $\theta$ - $2\theta$  XRD scans (Bragg-Brentano geometry) in which the scattering vector is maintained normal to the plane of the film, for Cr films prepared on (a) MgO(100), (b) MgO(110) with  $t = 40$  nm and (c) polycrystalline fused silica with  $t = 320$  nm.

$t$ (nm)	MgO(100)				MgO(110)			
	$a$ (Å)	FWHM (200)	$T_{\text{coh}}$ (nm)	Mosaic (200)	$a$ (Å)	FWHM (211)	$T_{\text{coh}}$ (nm)	Mosaic (211)
20	2.890	1.71°	11	1.71°				
40	2.886	0.79°	21	0.80°	2.885	0.58°	19	0.58°
80	2.886	0.81°	20	0.82°	2.890	0.84°	18	0.84°
160	2.886	0.40°	26	0.40°	2.890	0.34°	34	0.34°
320	2.888	0.50°	25	0.51°	2.889	0.57°	22	0.57°

**Table 1:** The measured out-of-plane full-width at half-maximum (FWHM) XRD parameters of the selected Bragg peak and the mosaic spread of this peak, for epitaxial Cr films of thickness  $t$  prepared at 800°C on MgO(100) and MgO(110) substrates, respectively. The coherence length,  $T_{\text{coh}}$ , was calculated using the Debye-Scherrer equation after removing the resolution of the instrument.

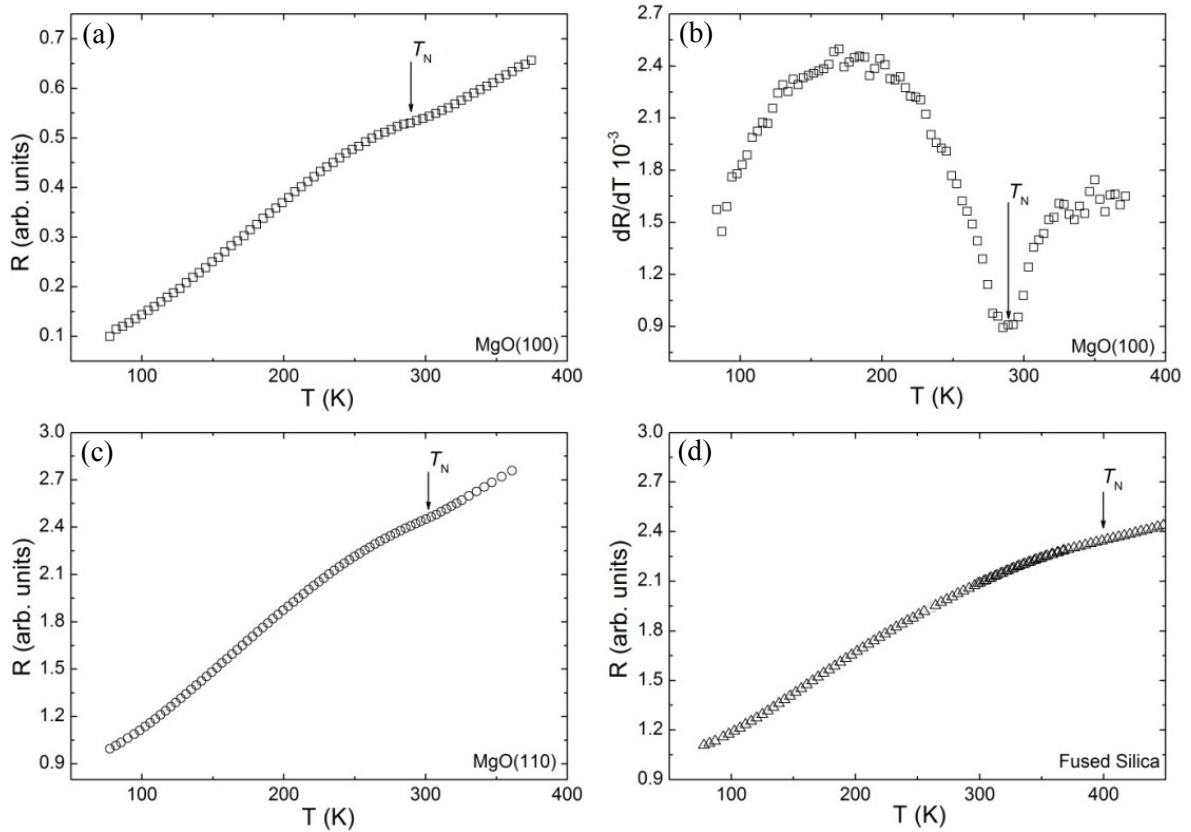


**Figure 2:** Resistance ( $R$ ) versus temperature ( $T$ ) graphs for Cr thin films prepared on the substrates: (a) MgO(100) with  $t = 160$  nm measured along [100], (c) MgO(110) with  $t = 40$  nm and (d) polycrystalline fused silica with  $t = 80$  nm. Figure (b) shows  $dR/dT$  versus  $T$  for the sample prepared on the MgO(100) with  $t = 160$  nm. The temperature associated with the minimum in the  $dR/dT$  versus  $T$  curves was taken as the Néel temperature ( $T_N$ ) as indicated by the arrows in all the curves.

This leads to a reduction in the number of charge carriers available for conduction resulting in an increase in resistivity just below  $T_N$  [1]. In general the samples prepared on the quartz shows much weaker anomalies at  $T_N$ , as is evident from the example shown in figure 2(d). This is attributed to the higher disorder that exists in these structures with them not being epitaxial [7].

The Néel temperature for Cr alloys can be defined either as the temperature of the minimum in  $R(T)$  accompanying the magnetic phase transition, or the inflection point in  $R(T)$  curve [1]. As the anomalies associated with the magnetic transitions in these samples were relatively weak, it was decided to refer to the second definition and  $T_N$  was determined by considering the  $dR/dT$  versus  $T$  curves and  $T_N$  taken as the temperature associated with the minima on these curves. This is one of the accepted methods generally used for the determination of  $T_N$  in Cr based thin films [9]. An example of this is shown in the figure 2(b) for the  $t = 160$  nm sample on MgO(100). It should however be mentioned that extrinsic morphology contributions that dramatically change the resistance, may bias obtained  $T_N$  values to some extent [8].

The variation in  $T_N$  as function of layer thickness,  $t$ , in the Cr thickness series is shown in figure 3 for the three substrates used. For the epitaxial films prepared on MgO(100), shown in figure 3(a), we observe an initial sharp decrease in  $T_N$  starting at a value of 320 K for the thinnest sample, to level off at a value of approximately 285 K for a sample of thickness 320 nm. Comparison with the literature reveals contrasting behaviours. Considering the resistivity versus temperature data of Kummamuru *et al.* [7] (see their figure 1(c)) for their Cr thickness series, also prepared on MgO(100), with  $17.5 \text{ nm} \leq$

$t \leq 350$  nm, the values for  $T_N$  value also decreased with increasing thickness, whereas Mattson *et al.* [9] observed  $T_N$  to increase from approximately 230 K approaching the bulk value at a thickness of approximately 300 nm.

For the epitaxial films prepared on MgO(110), a general increase in  $T_N$  approaching the bulk value for Cr is observed for increased thickness, as reported by [4, 9]. For this series the values for  $T_N$  is generally lower than that observed for layers prepared on MgO(100), starting at  $T_N \approx 230$  K for the thinnest sample, reaching a maximum value of 298 K at  $t = 80$  nm, where after  $T_N$  tends to level off at approximately 270 K for  $t \geq 160$  nm.

The  $T_N$  values obtained for the polycrystalline Cr thin films, deposited on the fused silica substrates are much higher compared to the epitaxial Cr films on MgO(100) and MgO(110) substrates, with  $T_N \approx 360$  K for the samples with  $t < 80$  nm and increasing to  $T_N \approx 460$  K for the sample with  $t = 320$  nm. This behaviour corresponds to that observed in Cr-Ru thin films prepared on polycrystalline fused silica [8]. The high  $T_N$  for  $t = 320$  nm is unexpected and cannot be explained. However, as was pointed out by Prinsloo *et al.* [8], it incidentally corresponds with  $T_N = 475$  K for the CSDW-P Néel transition induced in bulk Cr through stresses associated with cold working [2].

Previous studies [10] on polycrystalline Cr films, grown on Corning glass substrates, also showed significant increases in  $T_N$  values by up to 60 K above the observed bulk value of 311 K [1] for samples with  $t \leq 30$  nm. This was ascribed to tensile stresses in the films that arose, in part, from the grain boundaries [11, 12]. It is then possible that the polycrystalline films with a high density of grain boundaries may behave like a cold-worked sample, resulting in a high temperature CSDW-P transition for the Cr film on fused silica [12], whereas the epitaxial films will have different internal stresses [8].

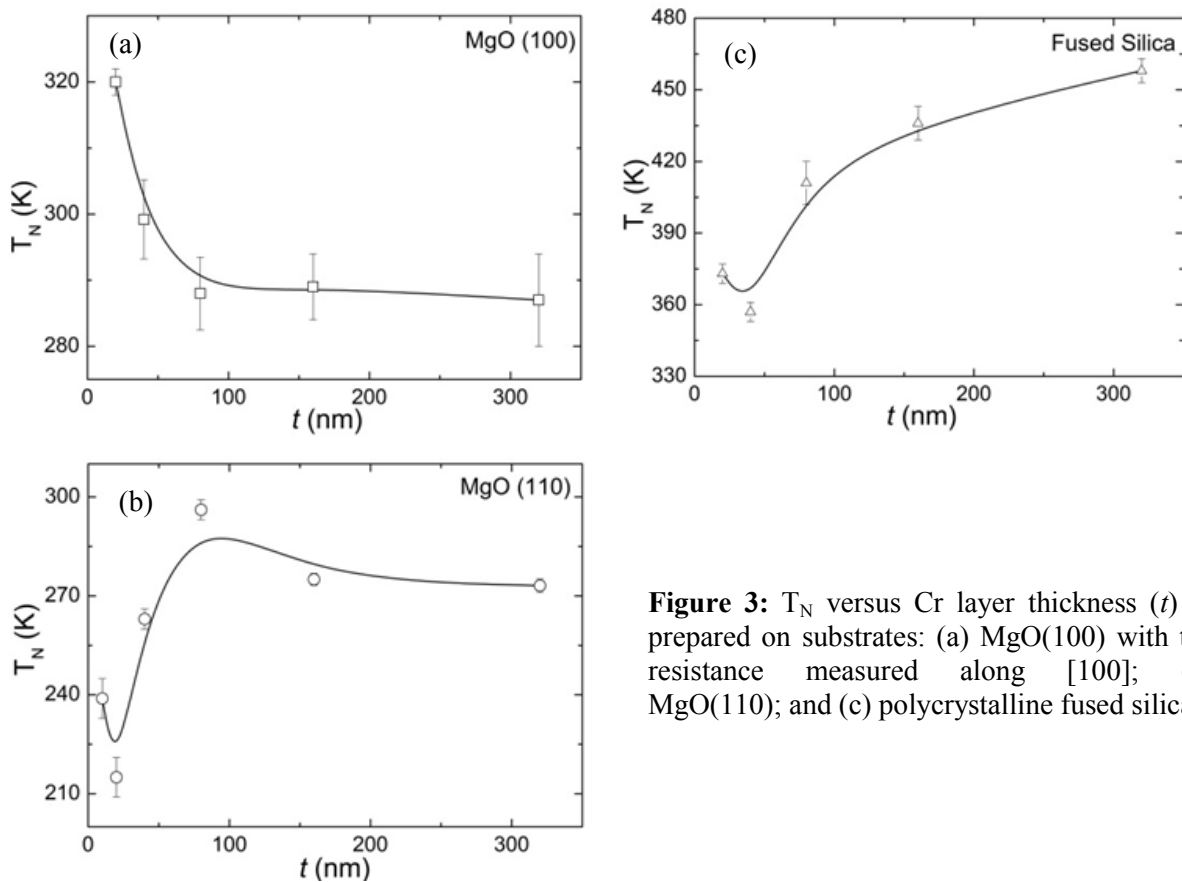


**Figure 3:**  $T_N$  versus Cr layer thickness ( $t$ ) as prepared on substrates: (a) MgO(100) with the resistance measured along [100]; (b) MgO(110); and (c) polycrystalline fused silica.

#### 4. Conclusions

The XRD characterization of Cr thin films prepared on MgO(100), MgO(110) and fused silica substrates, with thicknesses 20 nm to 320 nm, was used to determine the mosaicity and coherence length (along the growth direction) of the thin films. The results in general indicate a slight improvement in the layer quality with increase in sample thickness.  $T_N$  versus  $t$  graphs for the various substrates show an increase in magnetic transition temperature values with increase in thickness for the samples prepared on MgO(110) and fused silica substrates, whereas the opposite is observed for the MgO(100) samples. The relatively high  $T_N$  values obtained for the polycrystalline samples might be attributed to the presence of internal tensile stresses in the films that arise, in part, from the grain boundaries [11, 12].

The differences in the  $T_N - t$  behaviour of the epitaxial films prepared on the MgO(100) and MgO(110) substrates, as well as the high  $T_N$  values obtained for the polycrystalline samples warrants further investigation. As an extension of the present study, stress and strain analyses on these samples are planned to gain insight into these characteristics.

#### Acknowledgements

Financial support from the SA NRF (Grant Nos. 80928 and 80631) is acknowledged.

#### References

- [1] Fawcett E, Alberts HL, Galkin VY, Noakes DR and Yakhmi JV 1994 *Rev. Mod. Phys.* **66** 25
- [2] Fawcett E 1988 *Rev. Mod. Phys.* **60** 209
- [3] Zabel H 1999 *J. Phys. Condens. Matter* **11** 9303
- [4] Pierce DT, Unguris J, Celotta RJ and Stiles MD 1999 *J. Magn. Magn. Mater.* **200** 209
- [5] Fishman RS 2001 *J. Phys. Condens. Matter* **13** R235
- [6] Fullerton EE, Robertson JL, Prinsloo ARE, Alberts HL and Bader SD 2003 *Phys. Rev. Lett.* **91**(23) 237201
- [7] Kummamuru RK and Soh YA 2008 *Nature* **452** 859
- [8] Prinsloo ARE, Derrett HA, Hellwig O, Fullerton EE, Alberts HL and Van den Berg N 2010 *J. Magn. Magn. Mat.* **322** 1126
- [9] Mattson JE, Fullerton EE, Sowers CH and Bader SD 1995 *J. Vac. Sci. Technol. A* **13**(2) 276
- [10] Lourens JAJ, Aarjts S, Helbig HF, Cherlet L and Mehanna EA 1988 *J. Appl. Phys.* **63**(8) 4282
- [11] Windischmann H 1992 *Crit. Rev. in Solid State and Mat. Sci.* **17** 547
- [12] Boekelheide Z, Helgren E and Hellman F 2007 *Phys. Rev. B* **76** 224429